applied sciences

MDPI

Article

A Performance Analysis of a Hybrid OCDMA-PON Configuration Based on IM/DD Fast-OFDM Technique for Access Network

Hichem Mrabet [1,2]

[1] Department of IT, College of Computing and Informatics, Saudi Electronic University, Medina 42376, Saudi Arabia; h.mrabet@seu.edu.sa
[2] SERCOM-Lab., Tunisia Polytechnic School, Carthage University, Tunis 1054, Tunisia

Received: 21 July 2020; Accepted: 7 October 2020; Published: 30 October 2020



Abstract: The purpose of this article is to propose a new configuration based on OCDMA and Fast-OFDM techniques for access network applications. A hybrid intensity modulation with direct detection, fast orthogonal frequency-division multiplexing–code division multiplexing access (IM/DD Fast-OFDM-CDMA) system is analytically and numerically evaluated for an amplifier-free access network. Therefore, system performance is analytically investigated in terms of bit error rate/Q-factor as a function of simultaneous users, fiber length and launched optical power. Firstly, the proposed analytical model includes the overlapping effect among OFDM subcarriers, the peak-to-average power ratio (PAPR), and multiple access interference (MAI). Secondly, a simulation setup is performed, allowing four simultaneous users operating at 40 Gb/s in a passive optical network (PON) context. Furthermore, a power budget analysis is made between IM/DD Fast-OFDM-CDMA, all-optical IM/DD OFDM-CDMA (IM/DD AO-OFDM-CDMA) and OCDMA wavelength division multiplexing (OCDMA-WDM) configurations. It is shown that at 40 Gb/s and by using 2D-hybrid coding (2D-HC), the maximum achievable transmission-reach of IM/DD Fast-OFDM-CDMA is 142 km, which is 34 km and 60 km higher than those provided by the IM/DD AO-OFDM-OCDMA and OCDMA-WDM PON configurations, respectively.

Keywords: Fast-OFDM; optical CDMA; MAI; PAPR; access network; passive optical networks; security

1. Introduction

Orthogonal frequency-division multiplexing (OFDM) is an emerging technology in optical fiber communications due to its inherent advantages, which include simplified digital signal processing for channel estimation and the compensation of linear fiber-induced impairments, such as chromatic dispersion and polarization-mode dispersion [1]. OFDM is essentially a method of encoding digital data on multiple carrier frequencies, harnessing the (inverse) fast Fourier transform (IFFT) [2], and is widely used in wireless local area networks (802.11 a/g) and wireless metropolitan area networks (802.16 d). In the wireless domain, OFDM's advantages also include the support of several multiple access schema (e.g., time-division multiplexing access (TDMA), frequency-division multiplexing access (FDMA), code-division multiplexing access (CDMA)) and the compensation of multipath propagation [3,4]. In wireline communications, OFDM has been implemented in asynchronous digital subscriber lines (ADSLs) and digital video broadcasting (DVB). On the other hand, CDMA is a multiplexing scheme based on the user code signature with great potential for providing bandwidth allocation, maximization of network user capacity and security enhancement. Further, CDMA offers simple network management with great capacity to support asynchronous bursty traffic, low latency access, transparency to overlaid protocols and high network flexibility [5]. Hybrid OFDM-CDMA systems have been reported in the

literature using one dimensional (1D) codes, such as Walsh–Hadamard (WH), and mutually orthogonal complementary pairs (MOCP) in optical and wireless communication systems, respectively [6,7]. However, to increase the number of simultaneous users, the length of 1D codes should be increased, which results in higher decoding computational complexity. A practical solution to this issue is the employment of 2D codes by merging the 1D code structure and spatial/frequency hopping schema. Two-dimensional optical CDMA (OCDMA) codes have been implemented in the wavelength-division multiplexing (WDM) passive optical networks (PON) context [8–14].

The effectiveness of classical optical code-division multiplexing access (OCDMA) can be potentially improved by employing orthogonal frequency-division multiplexing (OFDM) with high-order quadrature amplitude modulation (QAM) in order to increase the spectral efficiency and signal capacity, while overcoming linear fiber impairments by simplified digital signal processing. In the state of the art, various hybrid systems based on 2D codes are proposed for OCDMA-PON, intensity modulation and direct detection OFDM-OCDMA (IM/DD OFDM-CDMA) [15,16], coherent optical OFDM-CDMA (CO-OFDM-CDMA) [17] and OFDM-SAC-OCDMA systems [18,19].

The Fast-OFDM technique is a spectral-efficient multicarrier modulation scheme based on reducing the subcarrier spacing. Thanks to the discrete cosine transform (DCT), the Fast-OFDM technique provides twice the bandwidth efficiency of the fast Fourier transform (FFT) used by the classical OFDM technique. Furthermore, Fast-OFDM is an emergent and cost-effective technique used to reduce the system complexity, and it has been widely applied in multimode fiber (MMF) [20,21] and single mode fiber (SMF) as well [22].

The aim of this research paper is to propose a new solution based on the combination of two technologies, such as OCDMA and Fast-OFDM, in order to increase the reachability distance in the context of access network applications. Then, we make a comparison between the proposed solution and other works proposed in the literature, to show the added value of the proposed solution in the PON configuration as a function of the allowed simultaneous users (cardinality), performance metrics (BER and Q-factor), systems components and reachability distance of the optical fiber link.

In this work, 2D codes and higher order modulation formats (i.e., m-order QAM) are combined into a hybrid IM/DD Fast OFDM-CDMA (IM/DD Fast-OFDM-CDMA) system for network access offering security and high spectral efficiency. To this end, a novel analytic model is developed to analyze system performance that includes key limitation parameters, such as OFDM subcarrier overlapping, peak-to-average power ratio (PAPR) and multiple access interference (MAI). Additionally, a 2D OCDMA code (2D-HC) is used in the proposed hybrid system at a signal bit-rate of 40 Gb/s and over 80 km of standard single-mode fiber (SSMF) link length, that has a split ratio of 1:16 and is amplifier-free. In our previous work reported in Refs. [15,23], we presented a numerical performance analysis of 40 Gb/s for the AO-OFDMA-OCDMA and OCDMA-WDM PON configurations, respectively. Numerical demonstrations revealed that the maximum achievable transmission-reach of the IM/DD Fast-OFDM-CDMA with 2D-HC coding for network access is 142 km, compared to 82 km and 108 km for the OCDMA-WDM and IM/DD AO-OFDM-CDMA PON configurations, respectively. To the best of our knowledge, it is the first paper to propose a hybrid system named IM/DD Fast-OFDM-CDMA for an amplifier-free access network, characterized by the inherent OCDMA security feature (i.e., by preserving the integrity component), Fast-OFDM's high spectral efficiency and IM/DD's cost-effective solution.

This paper is organized as follows: Section 1 presents the proposed IM/DD Fast-OFDM-CDMA system architecture for network access. In Section 2, the system model is analytically investigated. In Section 3, numerical simulation results are presented in terms of BER, Q-factor and power budget analysis. The last part deals with a budget analysis comparison.

2. IM/DD Fast-OFDM-CDMA System Architecture

Figure 1 depicts the architecture of the proposed Fast-OFDM-CDMA system based on a cost-effective IM/DD technique for an amplifier-free upstream PON configuration. The system architecture includes an optical line terminal (OLT), the SSMF channel, a coupler, and the optical network unit (ONU).

The data sent by the user to the ONU side is mapped to a symbol according to the selected constellation mapping schema (i.e., 16 QAM), then transferred to the Fast-OFDM subcarrier block for subcarrier selection. The total number of subcarriers selected for the system is equal to 64 subcarriers, but to meet the Fast-OFDM requirement only half of the frequency spacing among subcarriers is considered. Then, the mapped user signal from the Fast-OFDM subcarrier block is multiplied by the OCDMA signature generated by the OCDMA encoder, and sent to the optical modulator to convert the electrical signal to the optical one.

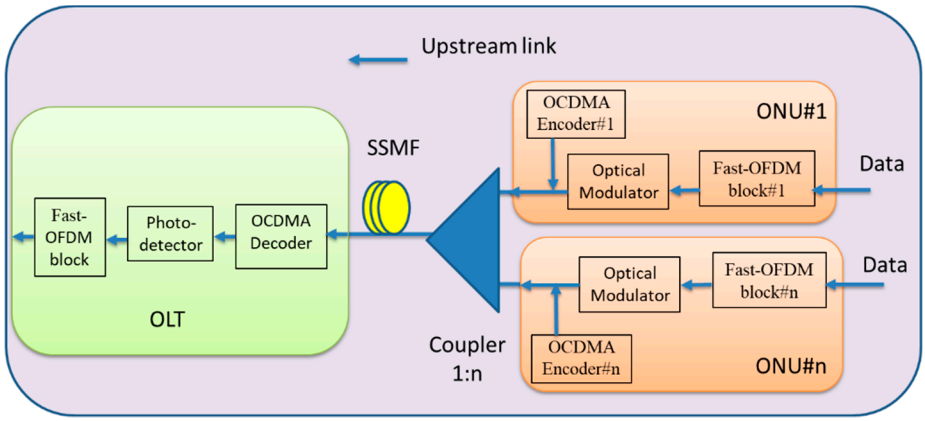


Figure 1. IM/DD Fast-OFDM-CDMA system architecture.

On the OLT block, the received signal is converted from optical to electrical thanks to the optical demodulator. Then, the generated signal is multiplied by the desired signature provided by the OCDMA decoder, and the Fast-OCDMA subcarrier decoder is applied to restore the symbol. Finally, the symbol is de-mapped to restore the emitted user data.

3. Analytical System Model

The signal-to-noise ratio (SNR) expression as a function of simultaneous PON users can be expressed as follows:

$$\mathrm{SNR} = \frac{S}{(K-1)\sigma^2 + N_0} \tag{1}$$

where S is the received signal (i.e., corresponding to the transmitted symbol) and σ^2 is the noise variance. In our model, the noise variance includes MAI and subcarriers overlapping, which can be defined as follows:

$$\sigma^2 = \sigma^2_{MAI} + \sigma^2_{overlap} \tag{2}$$

where σ^2_{MAI} is related to 2D-HC codes and given by [23]:

$$\sigma^2_{MAI} = \frac{H}{2P^2}\left(1 - \frac{H}{2P^2}\right) \tag{3}$$

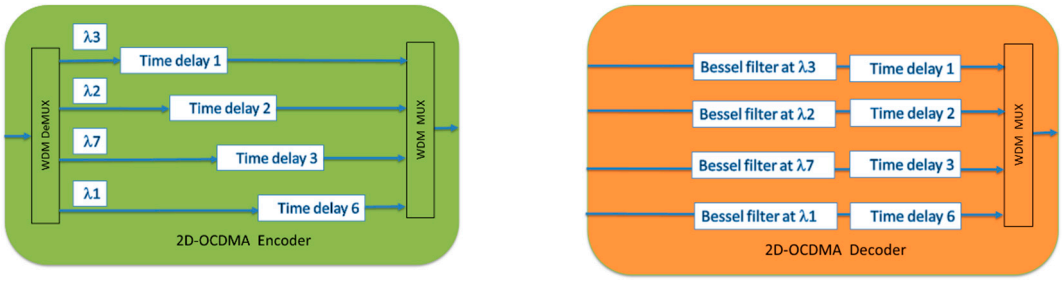
In Equation (3), H and P are the average probability hit of chips related to 2D-HC and the prime number, respectively. In this study, we also consider the photo-detector noise (N_0).

In fact, 2D-HC is built as follows: the maximum-length (ML) sequence is employed for the wavelength hopping, and the prime number is used for temporal spreading (i.e., examples of seven 2D-HC codes are described in Table 1, where {1, 2, 3, 4, 5, 6, 7} symbolize the wavelengths {λ_1, λ_2, λ_3, λ_4, λ_5, λ_6, λ_7} and [23]). The 2D-HC code is defined with respect to wavelength hoping H_j and temporal spreading S_i as shown in Table 1 the different code sequences S_iH_j where i vary from 0 to 4 and j vary from 0 to 3).

Table 1. Seven 2D-HC sequences with prime number equal to 7.

S_0H_1	30000000	20000000	70000000	00000000	00000000	10000000	00000000
S_2H_1	50000000	40000000	20000000	00000000	00000000	30000000	00000000
S_4H_1	20000000	10000000	60000000	00000000	00000000	70000000	00000000
S_1H_2	10000000	70000000	50000000	00000000	00000000	60000000	00000000
S_3H_2	40000000	30000000	10000000	00000000	00000000	20000000	00000000
S_0H_3	60000000	50000000	30000000	00000000	00000000	40000000	00000000
S_2H_3	70000000	60000000	40000000	00000000	00000000	50000000	00000000

Figure 2 represents the implementation of the OCDMA encoder and decoder based on the 2D-HC S_0H_1 sequence. As shown in Figure 2, the 2D-OCDMA encoder and decoder are composed of the WDM multiplexer, time delay, Bessel filter and WDM de-multiplexer.



(**a**) (**b**)

Figure 2. Implementation of 2D-HC for S_0H_1 sequence. 2D-OCDMA encoder based on S_0H_1 sequence (**a**); 2D-OCDMA decoder based on S_0H_1 sequence (**b**).

One major drawback related to single-band (SB) and multi-band (MB) OFDM systems is their sensibility to fiber nonlinear effects due to the high PAPR of OFDM signals [24]. In fact, even in SB OFDM, four-wave mixing (FWM) happens among electronic OFDM subcarriers due to its multi-carrier nature producing inter-subcarrier interference (ICI) [25]. As long as the cyclic prefix is a time-shifted copy of a part of the OFDM signal in the "observation" period, the transmitted time domain waveform inside this period for one OFDM symbol can be expressed by Equation (4):

$$s(t) = \sum_{k=1}^{N} X_k \, e^{\left(\frac{2\pi j(k-1)t}{T_s}\right)} \tag{4}$$

where X_k and N represent the input symbol and the subcarrier number of the classical OFDM symbol, respectively.

Since the frequency gap between subcarriers is reduced to half ($\frac{1}{2T_s}$) for the Fast-OFDM symbol, the signal becomes [26]:

$$s(t) = \sum_{k=1}^{N} X_k \, e^{\left(\frac{\pi j(k-1)t}{T_s}\right)} \tag{5}$$

The kth OCDMA encoder produces the user signature as follows:

$$s_k(t) = \sum_{l=1}^{F} P_T c_k(t - lT_c) \tag{6}$$

where F and T_c represent the code length and the time chip period, respectively.

At the input of the optical modulator, the electrical signal can be written as follows:

$$s(t) = \sum_{k=1}^{N} \sum_{l=1}^{F} P_T c_k(t - lT_c) X_k \, e^{\left(\frac{\pi j(k-1)t}{T_s}\right)} \tag{7}$$

In order to make a comparison between the transmitted signals in the cases of the Fast-OFDM-CDMA configuration and the AO-OFDM-CDMA and OCDMA-WDM systems, we introduce Equations (8) and (9), respectively, as follows:

$$s_1(t) = \sum_{k=1}^{N} \sum_{l=1}^{F} P_T c_k(t - lT_c) X_k \, e^{\left(\frac{2\pi j(k-1)t}{T_s}\right)} \tag{8}$$

where $s_1(t)$ represents the transmitted signal in the case of the AO-OFDM-CDMA configuration.

$$s_2(t) = \sum_{k=1}^{N} \sum_{l=1}^{F} P_T c_k(t - lT_c) X_k \tag{9}$$

where $s_2(t)$ represents the transmitted signal in the case of the OCDMA-WDM configuration.

Meanwhile, the PAPR is determined by Equation (8), as follows:

$$PAPR = \frac{max(|s(t)|^2)}{E(|s(t)|^2)} \tag{10}$$

where $max(|s(t)|^2)$ and $E(|s(t)|^2)$ are the maximum and the mean of the Fast-OFDM symbol, respectively.

A good way to characterize the PAPR is to use the complementary cumulative distribution function (CCDF) of Pc, which is expressed as Pc = Pr{PAPR > a_p}. Pc is defined as the probability that PAPR overtakes a particular value of a_p. In the latter case, the variance of subcarriers overlap is defined in Equation (11).

$$\sigma^2_{overlap} = P_r\{PAPR > a_p\} \tag{11}$$

The effects of PAPR and nonlinearities on the system performance are added through the variance of the OFDM subcarriers overlapping. In addition, we consider the particular case in Equation (10) in order to minimize PAPR and simplify the calculations.

$$\sigma^2_{overlap} = PAPR \tag{12}$$

The bit-error-rate (BER) expression is derived from the SNR expression in Equation (1), as follows [17]:

$$BER = \frac{2}{log_2(M)}\left(1 - \frac{1}{\sqrt{M}}\right) erfc\left(\sqrt{\frac{3SNR}{2(M-1)}}\right) \tag{13}$$

where M is defined as the modulation order.

4. Analytical Results

Table 2 shows the simulation parameters deployed for the continuous wave laser (CW laser) transmitter, the G.652 SSMF optical channel and the OCDMA signature parameters. Furthermore, to meet the high-standard optical communication system requirement, we consider forward error correction (FEC limit) and Q-limit for the BER and Q-factor metrics, respectively.

Table 2. Analytical system parameters.

Parameter	Value
Signal bit-rate	40 Gb/s
Modulation order	16 QAM
Cyclic prefix length	0.125
Data subcarrier number	64
Launched power, operating wavelength	10 dBm, 1550 nm
SMF attenuation	0.2 dB/km
Default SSMF length	80 km
CW laser spectral width ($\Delta\lambda$)	0.15 Mhz
2D-HC OCDMA code length	49
2D-HC OCDMA code weight	4
2D-HC OCDMA chip period	8.06×10^{-13}
2D-HC average probability hit of chips (H)	0.53

4.1. MAI Impact

Figure 3 presents the log(BER), as a function of simultaneous users, for the IM/DD Fast-OFDM-CDMA system compared to AO-OFDM-CDMA and OCDMA-WDM, while using 2D-HC codes.

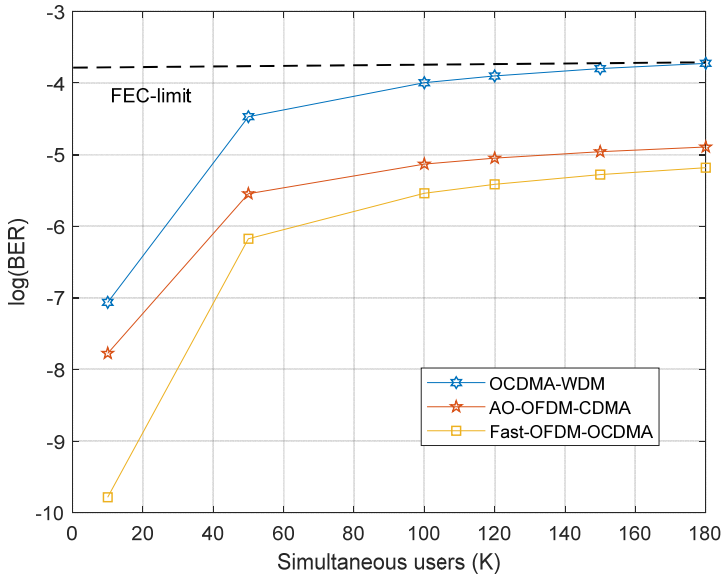


Figure 3. BER versus simultaneous users.

As shown in Figure 3, the three PON configurations can support up to 180 simultaneous users with a BER value less than $10^{-4.5}$ (i.e., less than the typical FEC limit of 3.8×10^{-3}) when 2D-Hybrid codes are used as the OCDMA signature. Furthermore, it is shown that the IM/DD Fast-OFDM-CDMA outperforms both the AO-OFDM-OCDMA and OCDMA-WDM systems in terms of BER as a function of simultaneous users. Further, at 100 simultaneous users, the IM/DD Fast-OFDM-CDMA configuration improves the system performance by factors of $10^{-0.5}$ and $10^{-1.5}$, in terms of BER, compared to AO-OFDM-OCDMA and OCDMA-WDM, respectively.

4.2. Fiber Length Effect

Figure 4 presents the log(BER) as a function of fiber length for the IM/DD Fast-OFDM-CDMA system compared to AO-OFDM-CDMA and OCDMA-WDM at 16 simultaneous users.

As demonstrated by Figure 4, the three PON configurations fulfill the FEC limit for a fiber length up to 180 km. Further, at an SSMF length of 100 km it is shown that the Fast-OFDM-CDMA system outperforms AO-OFDM-CDMA and OCDMA-WDM by $10^{-1.5}$ and 10^{-1} in terms of BER, respectively.

Finally, the Fast-OFDM-CDMA and AO-OFDM-CDMA systems present the same BER at a fiber length equal to 200 km.

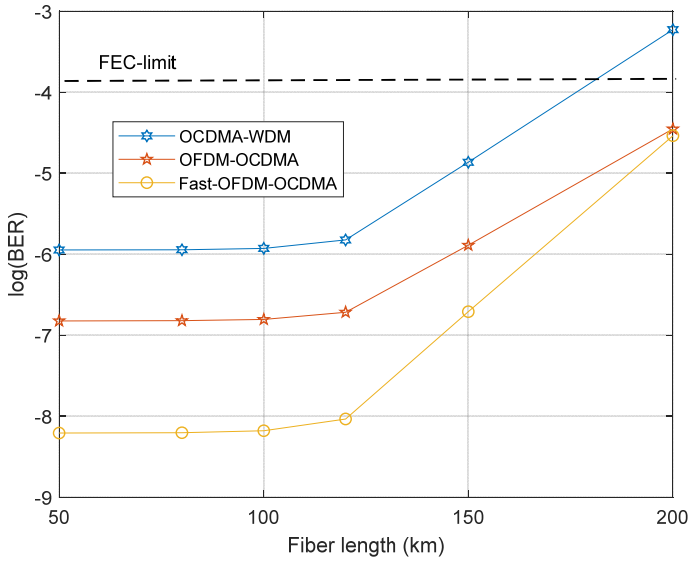


Figure 4. BER versus fiber length.

4.3. Optical Launched Power Effect

Figure 5 presents the log(BER) as a function of launched optical power for the Fast-OFDM-CDMA system compared to AO-OFDM-CDMA and OCDMA-WDM at K = 2. As depicted in Figure 5, the IM/DD Fast-OFDM-CDMA system outperforms both the AO-OFDM-CDMA and OCDMA-WDM PON configurations. Furthermore, it is shown that at a launched optical power of 0 dBm, the AO-OFDM-OCDMA and OCDMA-WDM systems have the same Q-factor, equal to 2.5 dB. However, at 0 dBm, Fast-OFDM-CDMA improves the system performance by a Q-factor equal to 2.5 dB compared to AO-OFDM-OCDMA and OCDMA-WDM. On one hand, AO-OFDM-CDMA has a better system performance compared to OCDMA-WDM, while the launched power is less than 0 dBm. On the other hand, for a launched optical power greater than 2 dBm, the OCDMA-WDM PON configuration upgrades AO-OFDM-CDMA in terms of Q-factor. Additionally, the latter PON configurations provide a Q-factor above the Q-limit (i.e., equal to 6 dB) when the optical launched power exceeds 4 dBm.

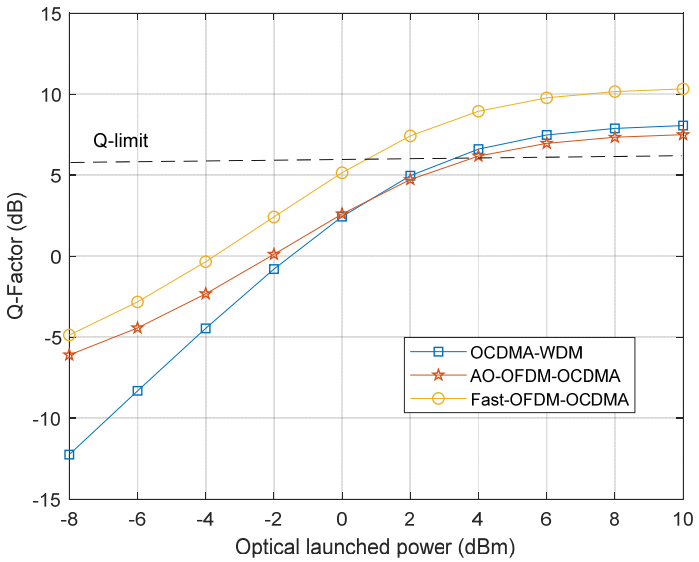


Figure 5. Q-factor versus launched optical power.

5. Numerical Results

Figures 6 and 7 represent the ONU and the OLT implementation, with the Optisystem simulator version 17, respectively.

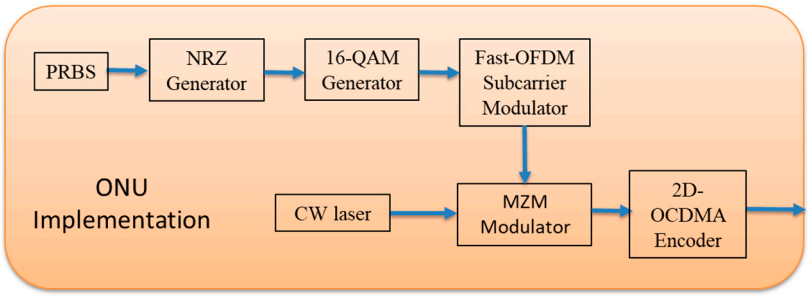


Figure 6. ONU implementation.

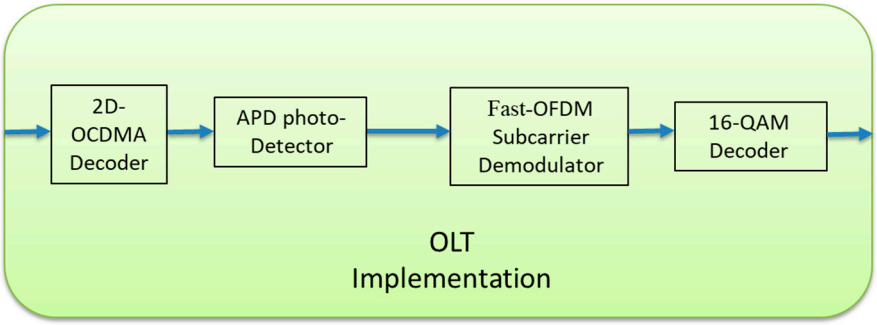


Figure 7. OLT implementation.

As shown in Figure 6, a pseudorandom binary sequence (PRBS) is used to generate a random bit user, then followed by an NRZ generator, followed by a 16-QAM generator and finally a Fast-OFDM subcarrier modulator is putted at the end of the first pipeline. A Mach–Zehnder modulator (MZM) is used to convert the electrical signal to an optical one based on a continuous wave (CW) laser source. The output signal of the MZM modulator will be multiplied by the signature generated by the 2D-OCDMA encoder. Finally, the output signal from the 2D-OCDMA encoder will be sent towards the optical channel.

On the OLT side, a 2D-OCDMA decoder is used to eliminate the user signature as depicted in Figure 7. Then, an APD photodetector is employed to convert the optical signal into an electrical one. In addition, a Fast-OFDM subcarrier demodulator followed by a 16-QAM decoder is useful to recover the received symbol as a user bit. In our simulation setup, the system provides 10 GHz spacing between 9 channels, with a 40 Gb/s signal capacity (25 GS/s sampling rate) per-channel, using 16-QAM. The OFDM block is composed of 64 electronic subcarriers (only 5 Ghz spacing among subcarriers is used thanks to the Fast-OFDM technique), a cyclic prefix of 2% to eliminate inter-symbol interference, 10 pilot subcarriers for carrier recovery and digital-to-analog/analog-to-digital converter clipping ratio, and quantization bits set at 13 and 10 dB, respectively. For Fast-OFDM-CDMA on this setup, 9 electrical subcarriers are also considered, supporting 4 simultaneous users in the network. The 5th middle channel is investigated, which suffers the most from nonlinear crosstalk effects, while the launched optical power per channel/optical subcarrier was fixed at the optimum 2 dBm for both cases of downstream link. The PRBS generated bits were 219-1, and hard-error decoding was performed at the receiver to calculate the BER. The CW laser, Fast-OFDM modulator, MZM modulator and related APD detector for IM/DD Fast-OFDM-CDMA were simulated at an aggregate bit rate of 40 Gb/s. The developed Fast-OFDM bloc, as well as the 2D-OCDMA block, was implemented in the Optisystem® simulator environment (electrical and optical components with SSMF). It should be noted that phase

noise and frequency offset have been considered here using three OFDM pilot subcarriers. Our system setup considered 1000 symbols per subcarrier. The adopted SSMF parameters for signal transmission over an 80 km length are the following: fiber nonlinear Kerr parameter, CD, CD-slope, fiber loss and differential group delay (DGD) of 1.1 $W^{-1}km^{-1}$, 16 ps/nm/km, 0.06 ps/km/nm^2, 0.2 dB/km and 0.2 ps/km, respectively. Likewise, in order to recover the phase after the photodetector, a low pass Bessel filter is used after the photodetector in the setup. In addition, a Bessel optical filter is employed before the photodetector at the third optical window to preserve the received signal phase shape.

As shown in Figure 8, the eye diagrams for four users generated by the Optisystem® BER analyzer are open, indicating the feasibility of our hybrid IM/DD Fast-OFDM-CDMA system in the PON context operating at 40 Gb/s. However, the eye becomes more closed when the number of users is raised; this is due to the MAI, which is considered as the most dominant degradation factor of OCDMA system.

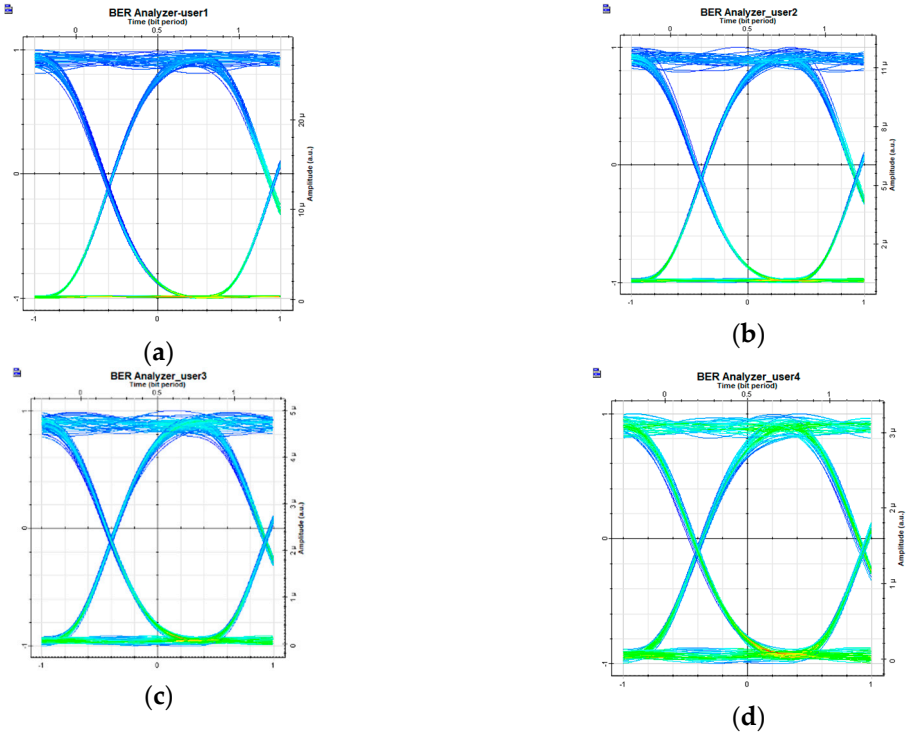


Figure 8. Eye diagrams: (**a**) for the first user; (**b**) for the second user; (**c**) for the third user; (**d**) for the fourth user.

6. Power Budget Analysis

The cost performance of the IM/DD Fast-OFDM-CDMA system is calculated as the optical power budget using an APD and a CW laser at OLT and ONU, respectively, as shown in Figure 9.

Table 3 presents the power budget calculation related to the proposed hybrid system configuration with 4 dBm and 15 dBm emitted average powers, corresponding to the local and long reach access network [27], respectively.

For the connector attenuation, four connectors are required in total to relay each component in the link, as shown in Figure 8 (i.e., a connector is needed to connect ONU, SSMF, splitter 1 × 16, SSMF and OLT), and if we consider that each connector has a loss of 0.4 dB [28], we get a total connector attenuation in the link in the order of 4 × 0.4 = 1.6 dB. In addition, each splitter 1 × 16 introduces a loss equal to 12 dB. On the one hand, it is shown that the maximum reachable distance between the ONU and OLT for the Fast-OFDM-CDMA system is equal to 112 km and 167 km for the lower case and the upper case, respectively. Likewise, we show that the proposed hybrid system can reach a long-reach PON distance of 167 km using an emitted average power of 15 dBm.

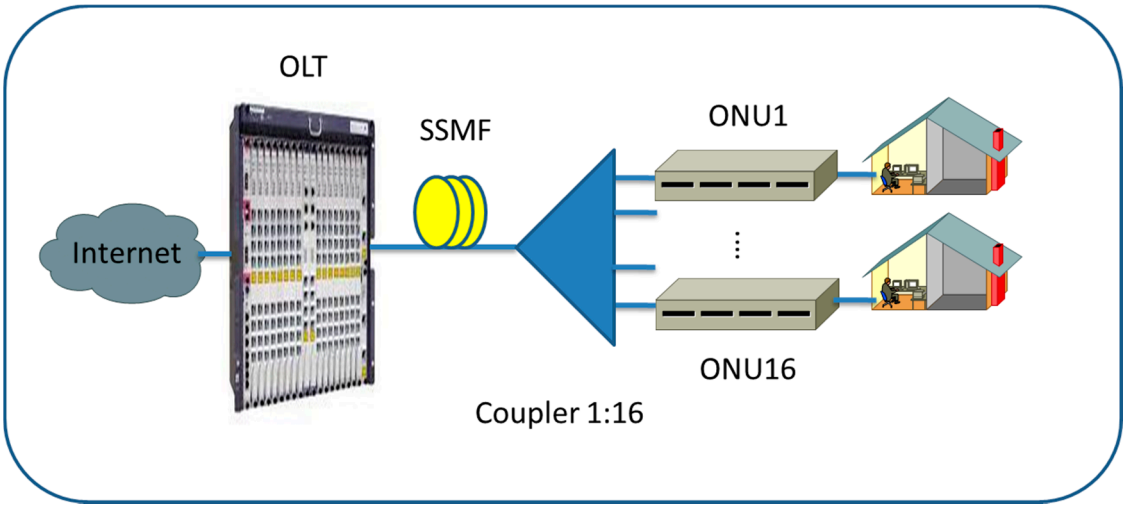


Figure 9. PON configuration used to perform power budget calculation.

Table 3. Budget power calculation.

	Lower Case	Upper Case
Emitted average power (dBm)	4	15
Connectors attenuation (dB)	−1.6	−1.6
Splitter attenuation (dB)	−12	−12
System margin (dB)	−3	−3
Received average power (dBm)	−(−35)	−(−35)
a = Available attenuation	22.4	33.4
Maximal distance between ONU and OLT($\frac{a}{\alpha}$)	112 km	167 km

Table 4 presents the power budget comparison related to the proposed hybrid system configuration compared to the OCDMA-WDM and AO-OFDM-CDMA systems.

Table 4. Budget power comparison.

Parameter	OCDMA-WDM	AO-OFDM-CDMA	Fast-OFDM-CDMA
Emitted average power (dBm)	15	10	10
Connectors attenuation (dB)	−3.6	−2.4	−1.6
Splitter attenuation (dB)	−27	−18	−12
System margin (dB)	−3	−3	−3
Received average power (dBm)	−(−35)	−(−35)	−(−35)
a = Available attenuation	16.4	21.6	28.4
Maximal distance between ONU and OLT($\frac{a}{\alpha}$)	82 km	108 km	142 km

Moreover, with a 10 dBm average launched optical power, our hybrid system increases the maximum achievable transmission reach to 142 km, compared to 108 km for AO-OFDM-CDMA. As a result, our hybrid Fast-OFDM-CDMA system can improve the total power budget with an increment equal to 6.8 dB (i.e., the power budget passed from 21.6 to 28.4 dB), as compared to the AO-OFDM-OCDMA PON configuration.

Table 5 summarizes the relevant 2D-OCDMA-PON systems. To make a fair comparison among our IM/DD Fast-OFDM-CDMA and the other proposed systems in the literature, we consider various features, such as the coding scheme, cardinality (i.e., number of users), performance measured metrics (i.e., BER and Q-factor), system components and reachability distance.

Table 5. Relevant 2D-OCDMA systems in PON configuration.

System	Coding Scheme	Cardinality	Performance	System Components	Reachability (km)
AO-OFDM-CDMA [15]	2D-HC	45	BER ≤ FEC limit	DFB + SMF + APD	108
2D-OCDMA [16]	2D-PHS 2D-HC	190 120	Q-factor = 6	DFB + SMF + APD	120 190
CO-OFDM-CDMA [17]	2D-PHS 2D-HC	16	BER ≤ FEC limit	VCSEL + SMF + APD	83.5
2D-OCDMA-WDM [23]	2D-HC	524	BER ≤ 10×10^{-10}	VCSEL + SMF + APD	82
IMDD OOFDM-CDMA [29]	2D-PHS	5	BER ≤ FEC limit	VCSEL + SMF + APD	80
2D-PV [30]	2D Permutation vectors' code	110	BER ≤ 10×10^{-9}	LED + SMF + PIN	20
IM/DD FAST-OFDM-CDMA	2D-HC	180	BER ≤ FEC limit	CWlaser + SMF + APD	142

As shown in Table 5, various 2D-OCDMA codes are proposed for PON applications, such as hybrid codes (2D-HC), prime hop system (2D-PHS) and 2D permutation vectors (2D-PV) codes. We can also see that when the bit rate is less than 40 Gb/s, the system authorizes a high cardinality, for instance in the 2D-OCDMA-WDM, 2D-OCDMA, 2D-PV and Fast-OFDM-CDMA PON configurations. Nonetheless, for a bit rate equal to 100 Gb/s, the number of simultaneous users is reduced to 5 and 15 for the IMDD OOFDM-CDMA and CO-OFDM-CDMA systems, respectively. As a conclusion, the IM/DD Fast-OFDM-CDMA system outperforms the AO-OFDM-CDMA, CO-OFDM-CDMA, IMDD OOFDM-CDMA and 2D-PV systems in terms of cardinality and reachability as well.

7. Conclusions

A 40 Gb/s IM/DD Fast-OFDM-CDMA system was analytically and numerically demonstrated using 2D-OCDMA HC codes for an amplifier-free access network. Our hybrid IM/DD Fast-OFDM-CDMA system was based on a breakthrough analytical model that accounts for OFDM subcarriers overlapping, MAI and PAPR. It was shown that our proposal outperforms both the IM/DD AO-OFDM-OCDMA and 2D-OCDMA-WDM PON configurations in terms of system performance. Indeed, at 0 dBm, IM/DD Fast-OFDM-CDMA improves the Q-factor by 2.5 dB compared to AO-OFDM-OCDMA and OCDMA-WDM. On the other hand, the numerical simulation results showed the implementation feasibility of our hybrid system operating at 40 Gb/s in the PON configuration via open eye diagrams. Power budget analysis revealed that at a launched optical power of 10 dBm and with 16 simultaneous users, our proposed technique can improve the total power budget by 6.8 dB compared to IM/DD AO-OFDM-OCDMA. This leads to an extension of the maximum achievable distance of up to 142 km, compared to 108 km and 82 km for IM/DD AO-OFDM-OCDMA and 2D-OCDMA-WDM, respectively. The future directions for the extension of the access network could be the integration of new emergent technologies, such as multi-meter waves [31] and time domain equalizers, based on the OFDM technique [32], to extend the reachability distance and integration of 5G/6G non orthogonal multi-access (NOMA) in order to connect local and metropolitan networks to the broadband global access network. Finally, although an access network based on the OCDMA-PON configuration preserves data integrity, securing the access network will be a big challenge for researchers in the near future, as regards preserving data confidentiality and privacy against various attacks and threats by using Blockchain technology (BCT) and machine learning (ML)-based solutions [33].

Funding: This research received no external funding.

Conflicts of Interest: The authors declare no conflict of interest.

References

1. Giacoumidis, E.; Mhatli, S.; Stephens, M.F.C.; Tsokanos, A.; Wei, J.; McCarthy, M.E.; Doran, N.J.; Ellis, A.D. Reduction of Nonlinear Inter-Subcarrier Intermixing in Coherent Optical OFDM by a Fast Newton-based Support Vector Machine Nonlinear Equalizer. *J. Lightwave Technol.* **2017**, *35*, 2391–2397. [CrossRef]
2. Mhatli, S.; Mrabet, H.; Dayoub, I.; Giacoumidis, E. A novel support vector machine robust model based electrical equaliser for coherent optical orthogonal frequency division multiplexing systems. *IET Commun. J.* **2017**, *11*, 1091–1096. [CrossRef]
3. Zhang, G.; de Leenheer, M.; Morea, A.; Mukherjee, B. A survey on OFDM-based elastic core optical networking. *Commun. Surv. Tuts.* **2013**, *15*, 65–87. [CrossRef]
4. Mao, T.; Wang, Z.; Wang, Q.; Chen, S.; Hanzo, L. Dual-Mode Index Modulation Aided OFDM. *IEEE Access J.* **2017**, *5*, 23871–23880.
5. Vardakas, J.S.; Moscholios, I.D.; Logothetis, D.; Stylianakis, G. Performance Analysis of OCDMA PONs Supporting Multi-Rate Bursty Traffic. *IEEE Trans. Commun.* **2013**, *61*, 3374–3384. [CrossRef]
6. Guo, X.; Wang, Q.; Zhou, L.; Fang, L.; Li, X.; Wonfor, A.; Penty, R.V.; White, I.H. 16-user OFDM-CDMA optical access network. In Proceedings of the Conference of Lasers and Electro-Optics (CLEO), San Jose, CA, USA, 5–10 June 2016.
7. Zhang, Z.; Tian, F.; Zeng, F.; Ge, L.; Xuan, G. Mutually Orthogonal Complementary Pairs for OFDM-CDMA Systems. In Proceedings of the International Conference on Signal Processing (ICSP), Hangzhou, China, 19–23 October 2014.
8. Yang, C. Spectral efficiency of the optical CDMA based-PONs using two-codes keying. *IEEE Commun. Lett.* **2010**, *14*, 767–769. [CrossRef]
9. Saghari, P.; Omrani, R.; Willner, A.E.; Kumar, P.V. Analytical Interference Model for Two-Dimensional (Time–Wavelength) Asynchronous O-CDMA Systems Using Various Receiver Structures. *J. Lightwave Technol.* **2005**, *23*, 3260–3269. [CrossRef]
10. Muciaccia, T.; Gargano, F.; Passaro, V.M.N. Passive Optical Access Networks: State of the Art and Future Evolution. *Photonics J.* **2014**, *1*, 323–346. [CrossRef]
11. Ahmed, N.; Rashid, M.A.; Islam, M. OCDMA/WDM system with DPSK modulation at 2.5Gbps for GPON application. In Proceedings of the 2nd Workshop on Recent Trends in Telecommunications Research (RTTR), Palmerston North, New Zealand, 1–3 February 2017.
12. Alves, T.A.B.; Durand, F.R.; Angelico, B.A.; Abrao, T. Power allocation scheme for OCDMA NG-PON with proportional–integral–derivative algorithms. *IEEE OSA J. Opt. Commun. Netw.* **2016**, *8*, 645–655. [CrossRef]
13. Mrabet, H.; Cherifi, A.; Raddo, T.; Dayoub, I.; Haxha, S. A Comparative Study of Asynchronous and Synchronous OCDMA Systems. *IEEE Syst. J.* **2020**, 1–12. [CrossRef]
14. Hadi, M.; Pakravan, M.R. Analysis and Design of Adaptive OCDMA Passive Optical Networks. *J. Lightwave Technol.* **2017**, *35*, 2853–2863. [CrossRef]
15. Mrabet, H.; Mhatli, S.; Dayoub, I.; Giacoumidis, E. Performance analysis of AO-OFDM-CDMA with advanced 2D-hybrid coding for amplifier-free LR-PONs. *IET Optoelectron.* **2018**, *12*, 293–298. [CrossRef]
16. Mrabet, H.; Dayoub, I.; Haxha, S.; Attia, R. Performance analysis of 2D-OCDMA system in long-reach passive optical network. *Opt. Laser Technol.* **2019**, *117*, 64–72. [CrossRef]
17. Mrabet, H.; Bahloul, F.; Amari, A.; Wen, Y.; Giacoumidis, E. Performance analysis of a hybrid 100G CO-OFDM-CDMA system with 2D signature for LR-PONs. In Proceedings of the ICTON 2020, Bari, Italy, 19–23 July 2020.
18. Yousif, B.; El Metwally, I.; Samra, A.S. A modified topology achieved in OFDM/SAC-OCDMA-based multi-diagonal code for enhancing spectral efficiency. *Photonic Netw. Commun.* **2019**, *37*, 90–99. [CrossRef]
19. Cherifi, A.; Yagoubi, B.; Bouazza, B.S.; Dahman, A.O. New Method for the Construction of Optical Zero Cross Correlation Code Using Block Matrices in OCDMA-OFDM System. *J. Telecommun. Electron. Comput. Eng.* **2016**, *8*, 33–39.
20. Giacoumidis, E.; Ibrahim, S.K.; Zhao, J.; Tang, J.M.; Ellis, A.D.; Tomkos, I. Experimental and Theoretical Investigations of Intensity-Modulation and Direct-Detection Optical Fast-OFDM over MMF-links. *IEEE Photonics Technol. Lett.* **2012**, *24*, 52–54. [CrossRef]

21. Giacoumidis, E.; Tsokanos, A.; Mouchos, C.; Zardas, G.; Alves, C.; Wei, J.L.; Tang, J.M.; Gosset, C.; Jaouën, Y.; Tomkos, I. Extensive Comparisons of Optical Fast-OFDM and Conventional Optical OFDM for Local and Access Networks. *IEEE OSA J. Opt. Commun. Netw.* **2012**, *4*, 724–733. [CrossRef]
22. Jarajreh, M.A. Reduced-Complexity Artificial Neural Network Equalization for Ultra-High-Spectral-Efficient Optical Fast-OFDM Signals. *Appl. Sci.* **2019**, *9*, 4038. [CrossRef]
23. Mrabet, H.; Dayoub, I.; Attia, R. A Comparative Study of 2D-OCDMA-WDM System Performance in 40G-PON Context. *IET Optoelectron.* **2017**, *11*, 141–147. [CrossRef]
24. Shieh, W.; Djordjevic, I. *OFDM for Optical Communications*; Elsevier: Amsterdam, The Netherlands, 2010.
25. Amari, A.; Dobre, O.A.; Venkatesan, R.; Kumar, O.S.S.; Ciblat, P.; Jaouën, Y. A survey on fiber nonlinearity compensation for 400 Gbps and beyond optical communication systems. *IEEE Commun. Surv. Tuts.* **2017**, *19*, 3097–3113. [CrossRef]
26. Wang, D.; Lei, C.; Luo, R.; Chen, H.; Chen, M.; Yang, S.; Xie, S. 16QAM optical fast-OFDM transmission system based on discrete fourier transform and frequency multiplexing. In Proceedings of the 2014 OptoElectronics and Communication Conference and Australian Conference on Optical Fibre Technology, Melbourne, Australia, 6–10 July 2014; pp. 445–446.
27. Matsumoto, R.; Kodama, T.; Shimizu, S.; Nomura, R.; Omichi, K.; Wada, N.; Kitayama, K. 40G-OCDMA-PON system with asymmetric structure using multi-port and sampled SSFBG encoder/decoders. *J. Lightwave Technol.* **2014**, *32*, 1132–1143. [CrossRef]
28. Brown, G. *The Optics Encyclopedia (Basic Foundations and Practical Applications)*; Wiley: Hoboken, NJ, USA, 2004.
29. Mhatli, S.; Mrabet, H.; Dayoub, I.; Giacoumidis, E. Performance evaluation of an IMDD optical OFDM-CDMA system. *Appl. Opt.* **2018**, *57*, 1569–1574. [CrossRef] [PubMed]
30. Yousif Ahmed, H.; Zeghid, M.; A.Imtiaz, W.; Sharma, T.; Chehri, A.; Fortier, P. Two-Dimensional Permutation Vectors' (PV) Code for Optical Code Division Multiple Access Systems. *Entropy* **2020**, *22*, 576. [CrossRef]
31. Hassan, K.; Masarra, M.; Zwingelstein, M.; Dayoub, I. Channel Estimation Techniques for Millimeter-Wave Communication Systems: Achievements and Challenges. *IEEE Open J. Commun. Soc.* **2020**, *1*, 1336–1363. [CrossRef]
32. Benieddi, A.; Elahmar, S.A.; Dayoub, I.; Haxha, S. Blind Adaptive Low-Complexity Time-Domain Equalizer for 100-Gb/s Direct-Detection Optical OFDM Systems Over Long-Reach SSMF. *IEEE Syst. J.* **2020**, 1–7. [CrossRef]
33. Mrabet, H.; Belguith, S.; Alhomoud, A.; Jemai, A. A Survey of IoT Security Based on a Layered Architecture of Sensing and Data Analysis. *Sensors* **2020**, *20*, 3625. [CrossRef] [PubMed]

Publisher's Note: MDPI stays neutral with regard to jurisdictional claims in published maps and institutional affiliations.



© 2020 by the author. Licensee MDPI, Basel, Switzerland. This article is an open access article distributed under the terms and conditions of the Creative Commons Attribution (CC BY) license (http://creativecommons.org/licenses/by/4.0/).